ALGERIAN JOURNAL OF ENGINEERING AND TECHNOLOGY

Algerian Journal of Engineering and Technology
ISSN: 2716-9227 (Print)
EISSN: 2716-9278 (Online)
DOI:
Oudjer et al / vol. 10, n°2 - 2025

Original Article Open Access

Recovery of uranium (VI) from aqueous effluents by an NaX zeolite and NaX modified by Na_2SO_4

Oudjer Faiza*[a], Khemaissia Sihem [a], Bendjeriou Fatiha [a], Khenich Ahmed Rami [a], Mohellebi Leila [a], Bennemla Messaoud [a], Kadi Hadil [b] and Boussouf Lila[b].

[a] *Draria Nuclear Research Center – CRND, Algiers, Algeria.*
[b] *Morsli Abdellah University Center, Tipaza, Algeria.*
* *Corresponding author Oudjer Faiza: f-oudjer@crnd.dz*
Article history: Received 01 September 2025, Revised 29 September 2025, Accepted 05 October 2025

ABSTRACT

This work aims to develop innovative materials that promote optimal uranium recovery. It focuses on the modification of NaX zeolite by sodium sulfate (Na_2SO_4) by hydrothermal means, then used as an adsorbent for uranyl ions. Analytical techniques such as X-ray diffraction, Fourier transform infrared spectroscopy, nitrogen adsorption-desorption and thermal analysis were used to characterize the structural and textural properties of the synthesize and modified material. The kinetics, adsorption isotherms and desorption cycle of NaX, NaX-Na_2SO_4 zeolites were studied to evaluate their potential for uranium adsorption. The experimental results indicate that the uranium adsorption capacity was improved from 23 mgU/g for NaX to 35 mgU/g for NaX-Na_2SO_4 in the concentration range of 10-300 mg/L in U, under the optimal conditions: pH 2.0, room temperature, initial concentration of 100 mg/L in U, (S/L) ratio of 10g/L and 7g/L, and contact time of 3h and 2h respectively for NaX and NaX-Na_2SO_4. The kinetic study revealed that the recovery of uranyl ions follows a pseudo-second-order model and the adsorption equilibrium data fit better to the Langmuir model for both materials. Desorption using 0,5 N HNO_3 solution resulted in approximately 90% recovery of uranyl ions after one treatment cycle using the modified NaX zeolite.

Keywords: Zeolite; NaX zeolite; sodium sulfate; uranium; adsorption; desorption.

Graphical abstract

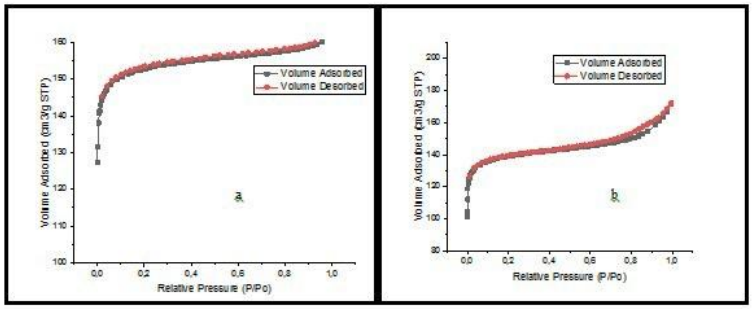

Adsorption-desorption of nitrogen (N_2) from zeolite (a) NaX and (b) NaX- Na_2SO_4.

Recommended Citation
Oudjer F, Khemaissia S, Bendjeriou F, Khenich AR, Mohellebi L, Bennemla M, Kadi H, Boussouf L. Recovery of uranium (VI) from aqueous effluents by an NaX zeolite and NaX modified by Na_2SO_4. *Alger. J. Eng. Technol. 2025*, 10(2): 32-43.

1. Introduction

Nuclear energy still accounted for almost 10% of global electricity and a quarter of low-carbon electricity, according to data presented in an annual IAEA publication [1]. Uranium is one of the most strategic elements in the field of nuclear energy production, used as the main fuel in nuclear reactors. The rapid growth of the nuclear industry has led to a significant increase in the production of aqueous effluents containing radionuclides, the management and treatment of which represent major challenges for environmental protection and resource security. Recovering uranium from these effluents is essential not only to reduce their toxicity and volume but also to ensure a more sustainable use of this resource.

Several processes are available for the recovery of uranium from aqueous solutions, but most of these techniques have some disadvantages, such as high operating costs, insufficient metal removal capacity, and the production of large sludge volumes [2, 3]. Adsorption using low-cost adsorbents and biosorbents is recognized as an efficient and economical alternative for the removal of heavy metals at low concentrations. Various materials, such as activated carbon, synthetic polymers, biomass, clay minerals, metal oxides, as well as a wide range of inorganic materials [2], including zeolites have been developed for the recovery of radionuclides [4].

Zeolites are microporous, natural or synthetic aluminosilicates characterized by a three-dimensional crystalline structure formed by interconnected microporous cages and channels [5-7]. These structures generate anionic sites through the presence of [AlO_2] units, with counter-cations (e.g, Na^+ and H^+) positioned near negatively charged AlO_4 tetrahedra to maintain charge neutrality [8]. These cations can be easily substituted by various other cations, including radioactive nuclides. This architecture gives these materials a high specific surface area as well as a significant cation exchange capacity and high thermal stability [9]. Zeolites have been widely used in nuclear waste management, particularly in the treatment of contaminated water following the Fukushima nuclear power plant accident [10]. In addition, the recycling and regeneration of adsorbed products are relatively easy. The long lifetime of these adsorbent solids is also a considerable advantage [11]. Among them, the NaX zeolite, belonging to the Faujasite group, is distinguished by a high ion exchange capacity, chemical stability and good accessibility to its active sites, which makes it an adsorbent of choice for the removal of uranyl ions (UO_2^{2+}) in aqueous media [12]. The open structure and the richness in exchangeable sodium ions facilitate interaction and exchange with uranyl ions, thus allowing efficient and rapid adsorption. Although they have a marked affinity for various contaminants, such as heavy metals and radionuclides, their adsorption capacity remains limited due to diffusional constraints linked to their microporous structure [2].

The adsorption of pollutants on the surface of zeolites depends on several factors, including mesoporosity, microporosity, and surface acidity [13]. Active sites, cavities, and channels play an important role in the adsorption performance of a zeolite material. An increase in the specific surface area leads to an increase in the number and size of active sites, cavities, and channels, thus allowing the adsorption of large quantities of pollutant molecules. Zeolites with different structures have specific affinities for different types of molecules. This affinity is determined by the size of the active sites/pores, cavities, and different Si:Al ratios (higher or lower) of the zeolite material, which favors the adsorption of pollutant molecules [14]. Various approaches have been proposed to generate additional porosity or property in zeolite crystals, either by post-synthesis such as ion exchange [15], dealumination [16] and desilication [17], or intra-synthesis such as the use of polymers, organic complexes, solid templates [18], ion exchange and impregnation, with the aim of improving the adsorption capacity of the zeolite towards uranyl ions which remains the most promising solution.

The objective of this work is to explore the chemical modification of NaX zeolite by intra-synthesis, by the addition of sodium sulfate (Na_2SO_4), in order to optimize its adsorption properties. This modification aims to increase the density and reactivity of the active sites, thus strengthening both the selectivity and the adsorption capacity towards uranium. The adsorption capacity of the developed and modified materials will be presented as dependent on certain experimental parameters such as the pH of the solution, the contact time, the solid-liquid ratio and the initial uranium concentration. Kinetic and isotherm studies of adsorption of uranyl ions on these materials will be undertaken.

2. Materials and Methods

2.1. Synthesis of NaX zeolite

The NaX zeolite was synthesized hydrothermally according to the following molar composition 4,54 Na_2O 3,44 SiO_2 Al_2O_3 180H_2O. The gel allowing the synthesis of the NaX zeolite is obtained according to the following protocol: In a

beaker containing a solution of water and NaOH, the necessary quantity of aluminum shavings is added under stirring until complete dissolution, followed by filtration. The silica source (sodium silicate) is added to the filtrate, the gel obtained is stirred for 2 hours and then introduced into the Teflon jacket of an autoclave for 24 hours of maturation. The autoclave is brought to an oven at 100°C for 6 hours, is then removed and soaked in cold water to stop crystallization. At the end of the synthesis, the product is filtered, washed with distilled water and dried at 80°C in an oven for 24 hours [19].

2.2 Synthesis of NaX zeolite modified by Na_2SO_4

The synthesis of NaX-Na_2SO_4 zeolite follows broadly the same steps as that of NaX zeolite. In a flask containing a solution of water and NaOH, the aluminum shavings are added under stirring until complete dissolution, after filtration the silica source is added, the mixture is subjected to stirring for 2 hours, where 3g of Na_2SO_4 [20] is added, it is then stirred for 30 minutes to ensure good homogenization. After this step the gel underwent a maturing step at room temperature, then introduced into an autoclave and placed in the oven at 100°C for 24 hours. The product of the synthesis thus recovered is filtered and washed with distilled water, then dried at 80°C for 24 hours.

2.3 Characterization

The synthesis products are analyzed by a PHILIPS X'PERT X-ray diffractometer with Cu-Kα (λ=1,5406 Å) in the range of 5-60° to identify the phases. The infrared spectra were recorded over a range of 400-4000 cm-1 by a Perkin Elmer UATR Two spectrometer. The specific surface area is determined by the BET method using the MICROMERITICS ASAP 2010 apparatus. The thermal analysis (ATG/ATD) was carried out on a SETARAM-LABSYS apparatus under nitrogen atmosphere, the heat treatment used is a temperature ramp from 25°C to 800°C.

2.4 Instrumentation

Uranium (VI) concentrations were determined by a UV-visible spectrophotometer (UV/Visible SAFAS MONACO UV mc Model). Adsorption experiments were performed by the batch protocol using a Jankel & Kunkel Ika-Werk HS 500 shaker. A Hanna Instrument model 2210 pH meter was used for pH reading. A Heraeus Lobofuge 601 centrifuge was used to separate the liquid from the material. A Prolabo drying oven was used to dry the prepared solids.

2.5 Reagents

A 1g/L stock solution was prepared by dissolving a quantity of uranyl nitrate salt $UO_2(NO_3)_2$ $6H_2O$ 99% in distilled water. Uranium solutions of 10 mg/L to 300 mg/L were prepared by appropriate dilutions. Arsenazo III, Sodium Silicate 99 %, Metallic Aluminum 100%, Sodium Sulfate 99%, Nitric Acid 65%, Hydrochloric Acid 37 %, Sodium Hydroxide 99%, Paranitrophenol, Ethylene Diamine Tetraacetic Acid 99%, Chloroacitic Acid 99%.

2.5 Adsorption experiment

The different experiments are carried out in closed polyethylene flasks of 100 mL capacity where we introduce 0.1 g of the materials NaX and NaX-Na_2SO_4. To each flask, we add a volume of 10 mL of the synthetic uranyl nitrate solution. The mixture is subjected to agitation using a shaker at room temperature. The two phases are separated by centrifugation. The obtained filtrates are analyzed by UV/Visible spectrophotometry using the Arsenazo III method [21-23] at 652 nm. The calculation of the uranium adsorption efficiency is given by the following formula:

$$\%\ \text{of Adsorption} = \left[\frac{C_0 - C_f}{C_0}\right] \times 100 \qquad (1$$

C_0 and C_f represent the initial and final uranium concentrations in the solutions (mg/L), respectively. The adsorption capacity Qe is calculated from the following equation:

$$Q_e = (C_0 - C_e) \times \frac{V}{m} \qquad (2$$

Ce: this is the equilibrium concentration of uranium (mg/L), V: this is the volume of the solution (mL) and m: this is the mass of the adsorbent (g).

3. Results and discussion

3.1. Characterization of the developed adsorbents

The XRD spectra of the elaborated NaX and NaX-Na_2SO_4 zeolites are shown in Figure 1. The diffractograms are

compared with that of the NaX structural type. The diffractogram of the elaborated NaX zeolite is typical of a faujasite X crystal structure [24].

The phases obtained are indeed of the NaX type, the diffraction lines located at 2θ respectively at 6,43°; 10,31°; 12°; 15,76°; 18,72°; 20,40°; 21,23°; 22,74°; 23,61°; 26,97°; 29,57°; 30,62° and 31,30° are characteristic of the NaX zeolite [25] and appear clearly on the diffractogram of the NaX material. The figure also shows that the NaX-Na_2SO_4 zeolite has a diffractogram similar to that of the NaX zeolite, with the exception of a notable decrease in the intensity of the diffraction lines. The addition of Na_2 SO_4 did not alter the crystal structure of the zeolite, but appears to have reduced the crystallization rate of the formed crystals [26]. The weakening of the line intensities of the modified zeolite shows that the crystallinity was reduced [27].

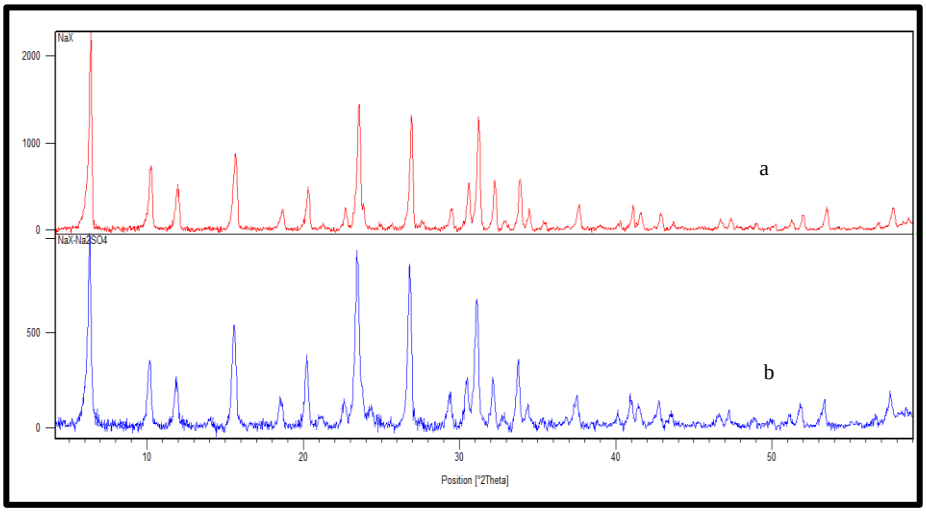

Fig 1. XRD patterns of the (a) NaX and (b) NaX-Na_2SO_4 zeolites.

The FTIR analysis result is shown in Figure 2. The characterization of NaX and NaX-Na_2SO_4 zeolites by infrared spectroscopy showed us that both materials have the same absorption bands, and reveal the characteristic structural absorption bands of zeolites. The absorption band at 457 cm^{-1} for NaX and 458 cm^{-1} for NaX-Na_2SO_4 is due to the internal vibrations of the (Si, Al) O_4 tetrahedron of zeolite X [28]. The absorption band at 750 and 751 cm^{-1} represents the symmetric stretching of Si-O-Si bonds. The absorption band at 984 and 1000 cm^{-1} represents the asymmetric stretching of Si-O-Al bonds in the regions [29]. The vertex vibration of the tetrahedra (DR6) appeared at 561 and 559 cm^{-1} which originates from external vibration of Al(Si)-O-Si and the symmetric elongations of the Al-O bonds which appear at 668 and 667 cm^{-1} [30]. The absorption bands observed at 1645 cm^{-1} attributed to the vibrations of the H-O-H bonds of water molecules [31]. The absorption bands observed at 3458 cm^{-1} attributed to the vibrations of the Si-OH groups, which represent the silanol groups [32, 33]. The broader band at 3447 cm^{-1} for NaX–Na_2 SO_4 indicates an increase in hydrogen interactions and a greater diversity of environments for the Si–OH groups, probably induced by the sodium sulfate modification.

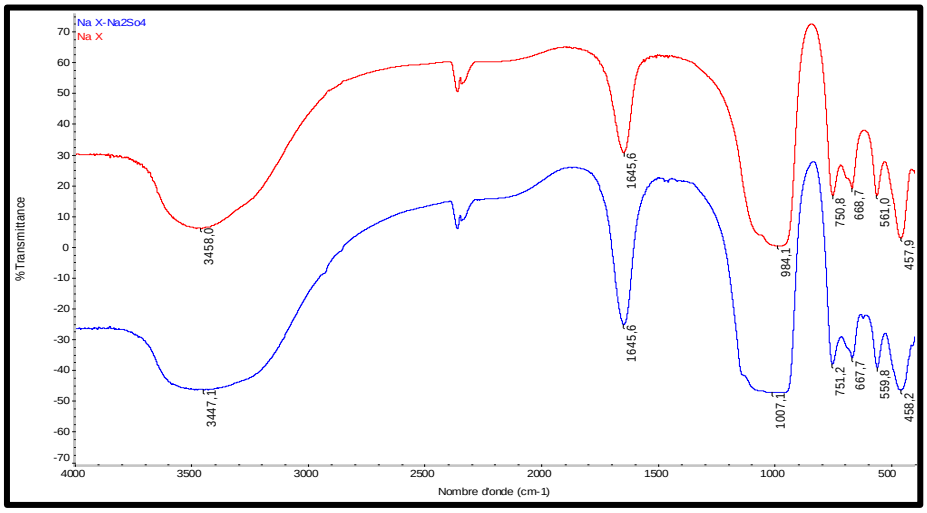

Fig 2. FTIR of the NaX and NaX-Na_2SO_4 zeolites.

Nitrogen adsorption-desorption analysis showed that both NaX and NaX-Na_2SO_4 materials exhibit type I and II isotherm curves respectively as shown in Figure 3, according to the IUPAC (International Union of Pure and Applied Chemistry) classification [34]. The occurrence of the H_4 type hysteresis loop in the pressure range of 0.7 to 1 P/P_0 for the NaX-Na_2SO_4 zeolite indicates that in addition to the microporous structure, there is also a small amount of mesopore [35], this hysteresis is more pronounced for the NaX-Na_2SO_4 material, which is probably formed during the modification by sodium sulfate. We notice a slight decrease in the specific surface area from 593 m^2/g of NaX material to 554 m^2/g for NaX-Na_2SO_4, and the pore volume of NaX-Na_2SO_4 decreased compared to that of NaX, decreasing from 0.20 to 0,18 cm^3/g.

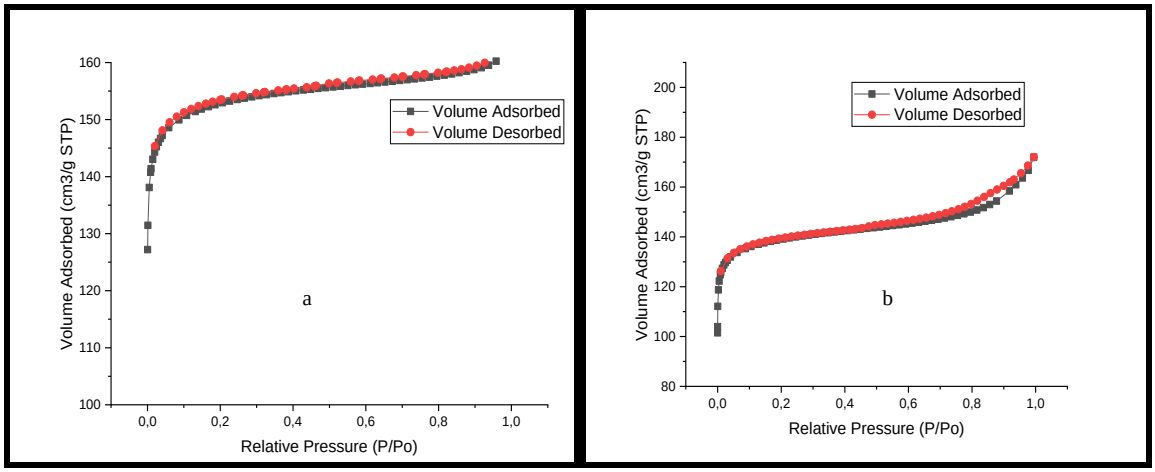

Fig 3. Adsorption-desorption of nitrogen (N_2) from zeolite (a) NaX and (b) NaX- Na_2SO_4.

The thermogravimetric curve of the NaX and NaX-Na_2SO_4 zeolites presented in Figure 4 allowed observing total mass losses between 50°C and 800°C, on the order of 22% for the zeolite NaX and 15% for the material NaX–Na_2 SO_4 . These losses are mainly attributed to the desorption of water molecules trapped in the pores of the zeolites, particularly in the temperature range from 50°C to 300°C. No significant mass loss was detected beyond 350°C, indicating that both materials retain good thermal stability up to 800°C [36]. This behavior is in agreement with previous results reported for an X zeolite, which also presented a total mass loss of 22% [37]. The incorporation of Na_2 SO_4 into the structure of the NaX zeolite led to a reduction in its hydrophilic nature, reflected by a 30% reduction in water-related mass loss.

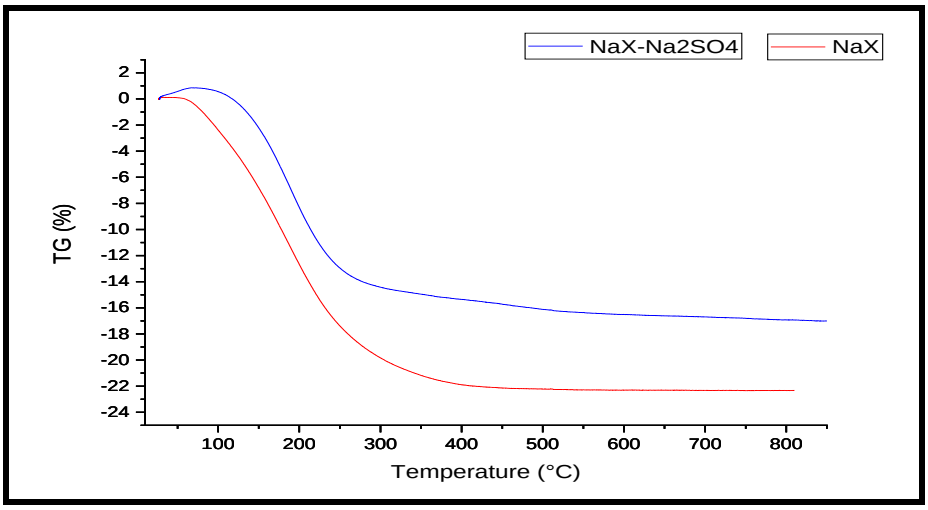

Fig 4. Thermograms of NaX and NaX-Na_2SO_4 zeolites.

3.2. Effect of pH on uranium adsorption

In order to evaluate the pH influence of uranium adsorption on NaX and NaX-Na_2SO_4 zeolites, we varied the pH of the solution from 1,5 to 9. The results of the experiments are illustrated in Figure 5.

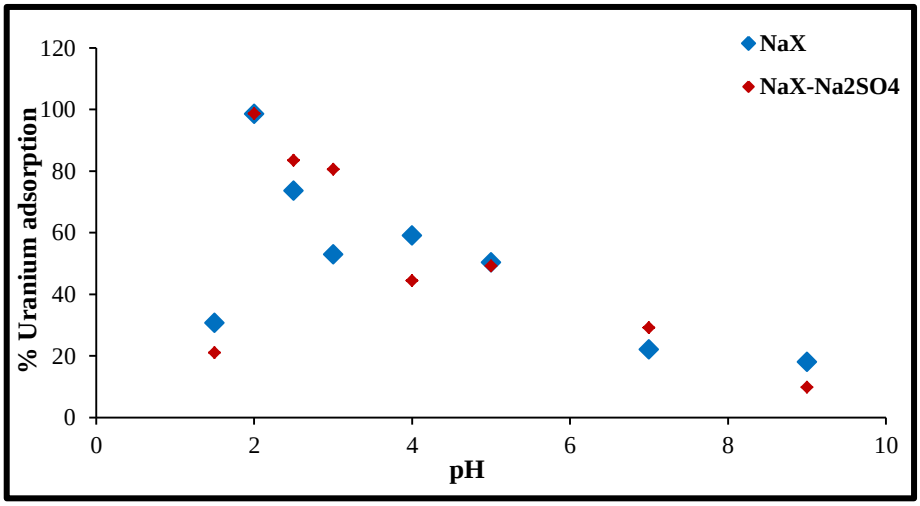

Fig 5. Effect of pH on uranium adsorption by NaX and NaX-Na_2SO_4 materials: temperature 21±2°C; [U]=100 mg/L, contact time=5h, S/L ratio=10 g/L.

The uranium recovery rate by both adsorbents is much higher at acidic pH, reaching the maximum at pH 2 for NaX and NaX-Na_2SO_4, hence the adsorption percentage is 98,51% for the NaX zeolite and 98,68% for the NaX-Na_2SO_4 zeolite. This evolution can be explained by the fact that at low pH values, adsorption is unfavorable, this is due to the competing H^+ ions which are in competition with the uranyl ions, their small size and their high mobility are favored to occupy the active sites of the adsorbent [38]. In the pH range 2-5, various monometric and polymetric hydrolyzed species of UO_2^{2+} are formed, these include: UO_2^{2+}, $(UO_2)OH^+$, $(UO_2)_2(OH)_2^{2+}$,$UO_2(OH)^{5+}$ [39]. At pH 5 $UO_2(OH)_2.H_2O$ is the major species, indicating that uranium removal could be a combination of adsorption and precipitation [40]. The decrease in adsorption for pH above 5 could be attributed to the formation of negatively charged soluble uranium complexes with lower adsorption affinity, such as $UO_2(OH)^{3-}$, $UO_2(OH)_4^{2-}$, $(UO_2)_3(OH)^{7-}$ since the electrostatic force between uranium complexes and zeolites is negligible [41].

3.3. Effect of solid-liquid ratio on uranium adsorption

The effect of varying the adsorbent (S)/adsorbate (L) ratio on uranium adsorption is shown in Fig. 6. For the study of this parameter, the ratio (solid/liquid) of the materials prepared was varied to 3g/L, 5g/L, 7g/L and 10g/L 15g/L. The

adsorption of uranyl ions increases with increasing adsorbent quantity, this can be attributed to an increase in the surface area and available adsorption sites of uranyl ions with increasing adsorbent quantity. The adsorption percentages reach a maximum at S/L ratios of 10g/L for NaX zeolite with an adsorption percentage of 98% and 7g/L for NaX-Na_2SO_4 with an adsorption percentage of around 96,70%. Beyond these values, a plateau forms, reflecting a stabilization of the adsorbed quantity, a sign of the saturation of the active sites during the adsorption process [42].

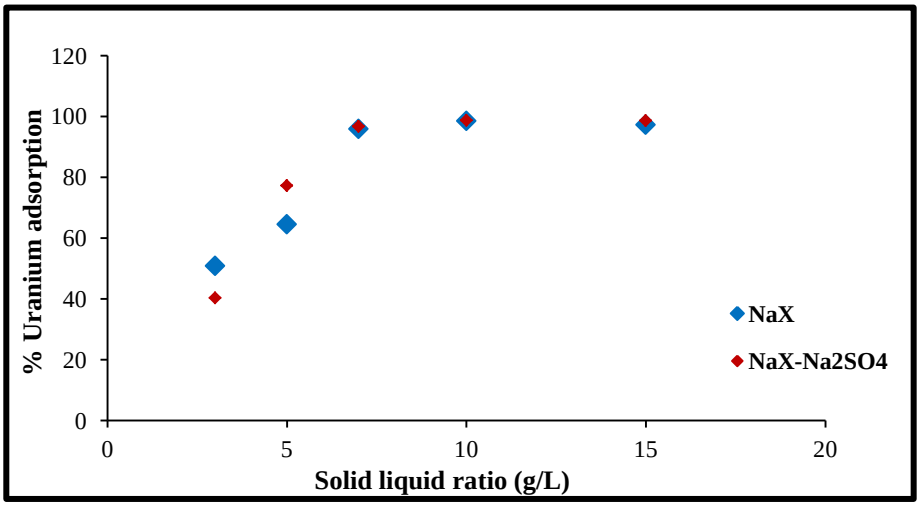

Fig 6. Effect of solid/liquid ratio on uranium adsorption by NaX and NaX-Na_2SO_4 materials: [U]=100 mg U/L, pH=2, Contact time=5h, Temperature 21±2°C.

3.4. Effect of contact time on uranium adsorption

The effect of contact time on the adsorption of uranyl ions on the two materials was studied over a time interval ranging from 2 to 300 min (Figure 7). It is observed that increasing the contact time from 2 to 180 minutes results in a progressive increase in adsorption, linked to the gradual filling of the active sites on the adsorbent. The adsorption efficiency is 95% for the NaX zeolite after 180 minutes and is 96% for the NaX-Na_2SO_4 after 120 minutes of contact. Beyond these durations, the kinetic curves of the NaX and NaX-Na_2SO_4 adsorbents reach a plateau. The kinetic study reveals that the adsorption process of uranyl ions involves two distinct fast and slow stages [43]: the first fast phase, due to the high adsorption affinity in the accessible pores, followed by a slower phase corresponding to the internal penetration of the ions, which controls the overall adsorption rate. After these two stages, equilibrium is reached.

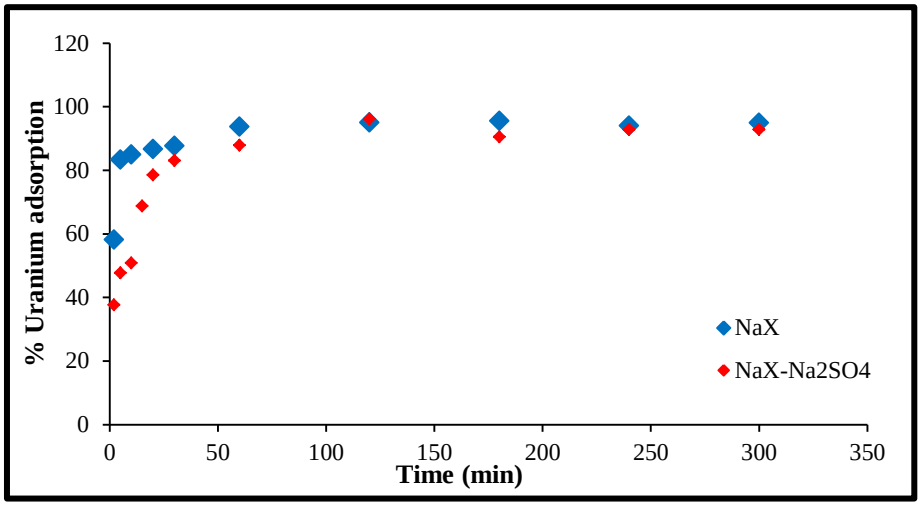

Fig 7. Effect of contact time on uranium adsorption by processed materials: [U]=100 mg U/L, pH=2, S/L ratio=10g/L NaX and 7g/L NaX-Na_2SO_4, Temperature 21±2°C.

3.5. Effect of initial uranium concentration on adsorption

The effect of varying the initial uranium concentration on the adsorption rate in the range of 10-300 mg/L by both adsorbents is shown in Figure 8. The adsorption percentage decreases with increasing initial uranium concentration, from 97% to 92% for NaX and from 97% to 88% for NaX-Na_2SO_4, this could be attributed to the strong interaction of uranyl ions (UO_2^{2+}) with the active sites of the adsorbent [44], as the uranium concentration increases the active sites of the adsorbent gradually saturate, limiting the adsorption capacity and thus reducing the relative adsorption percentage [45].

The uranium adsorption capacity Qe of uranium on both materials increased with increasing uranium concentration until reaching the maximum of 23 mgU/g for NaX zeolite and 35 mgU/g for NaX–Na_2 SO_4 material. This significant improvement in adsorption capacity for the modified zeolite indicates that Na_2 SO_4 modification enhanced the uranium adsorption performance. (See Figure 9).

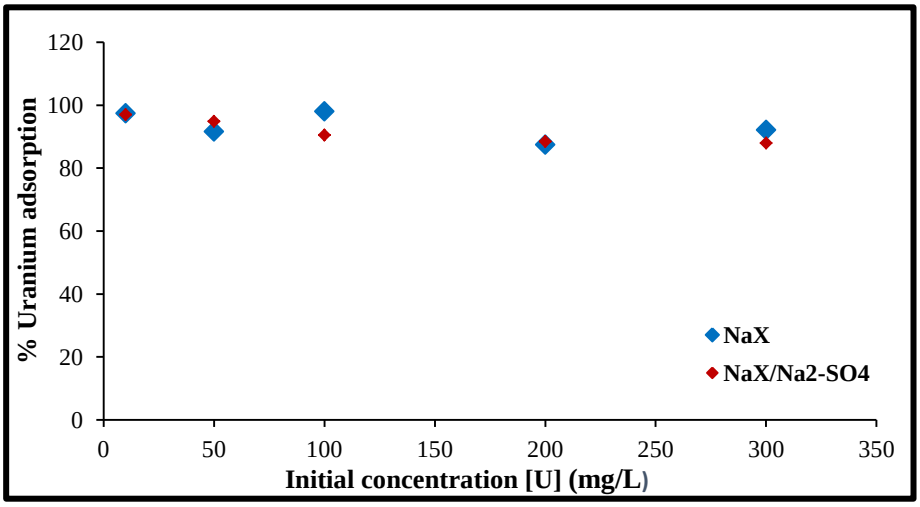

Fig 8. Effect of initial uranium concentration on adsorption by NaX and NaX-Na_2SO_4 materials : pH=2 ; S/L ratio =10g/L, Contact time =180min for NaX et 7g/L, Contact time =120min for NaX-Na_2SO_4 ; Temperature 21±2°C.

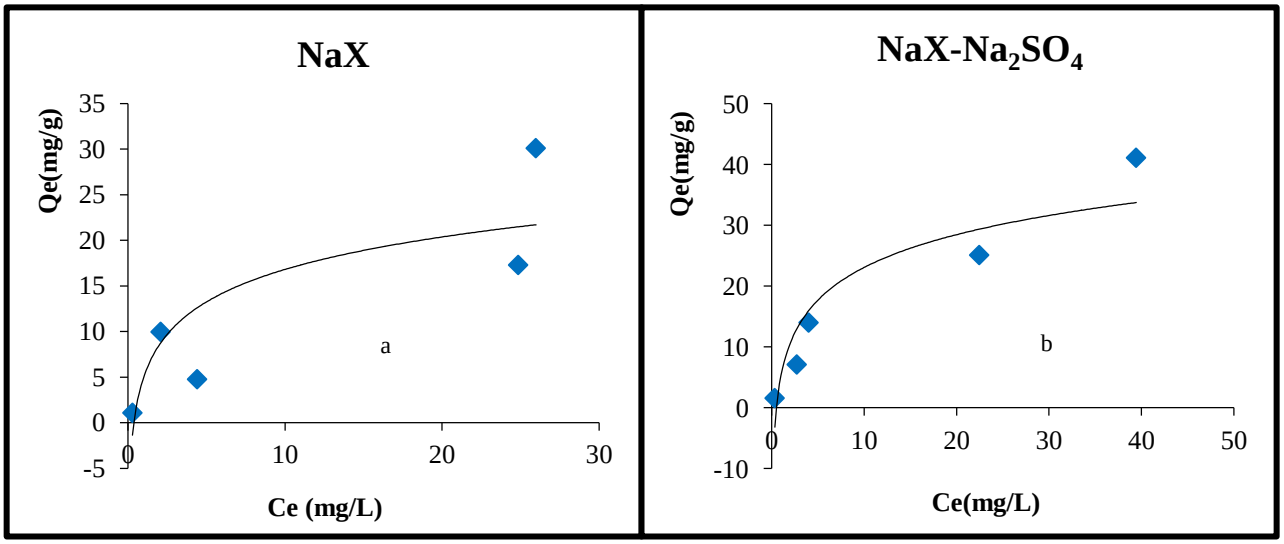

Fig 9. Variation of adsorption capacity as a function of the equilibrium concentration of uranium for the materials produced: zeolites (a) NaX and (b) NaX-Na_2SO_4.

3.6. Modeling of adsorption isotherms

The sorption isotherm depends on some parameters by which the experimental values express the surface properties of the materials and the affinity of the adsorbent, also give an idea about the distribution of metal ions between the solid/liquid

interface at equilibrium. The latter has been studied by different models such as Langmuir [46], Freundlich [47] and Dubinin-Radushkevich (D-R) [48] models. The characteristic constants of each model are grouped in Table 1.

Table 1. Correlation coefficients and adsorption parameters deduced from the Langmuir, Freundlich and Dubinin-Rudushkevich models after adsorption of UO^{+2} on NaX, NaX-Na_2SO_4 zeolites.

Adsorbent	Freundlich model			Langmuir model			Dubinin-Radushkevich model			
	K_f (mg/g)	n	R^2	Q_{max} (mg/g)	KL (L/mg)	R^2	Q_{max} (mg/g)	K (mol/L)	Ea (KJ/Mol)	R^2
NaX	2,99	1,577	0,856	19,157	0,209	**0,971**	$9,9.10^{-4}$	5.10^{-9}	**10**	0,864
NaX-Na_2SO_4	3,71	1,498	0,967	30,769	0,155	**0,995**	$1,68.10^{-3}$	5.10^{-9}	**10**	0,979

The experimental data are correlated by Langmuir, Freundlich and D-R isotherms to reveal the relationship between different materials and uranium (Table 1). According to the values of the correlation coefficients R^2 of the three models, the Langmuir model is the most suitable, which indicates that the adsorption is done on a homogeneous surface [49] with identical adsorption sites and formation of a monolayer of uranium on the surface of zeolites. According to the adsorption energy Ea found by Dubinin-Radushkevich model [50], to be 10 KJ/mol (higher than 8 KJ/mol), the adsorption of uranyl ions on the prepared materials is of chemisorption type.

3.7. Study of the kinetics of uranium adsorption on the developed materials

The results obtained from the contact time experiment are used to simulate the adsorption kinetics and explain the mechanism driving the adsorption process of uranium on NaX and NaX-Na_2SO_4 materials. In this regard, two kinetic models including pseudo first order and pseudo second order [51,52] are used. The pseudo-first order and pseudo-second order parameters for both adsorbents are grouped in Table 2.

Table 2. Values of kinetic parameters of uranium adsorption by the developed adsorbents.

Adsorbent	Pseudo first ordre			Pseudo secondordre			
	Q (mg/g)	K_{1ads} (min^{-1})	R^2	Qe (mg/g)	K_{2ads} (min^{-1})	h	R^2
NaX	1,878	0,032	0,918	9,775	0,0818	7,815	**0,999**
NaX-Na_2SO_4	7,432	0,035	0,869	13,717	0,0159	3,008	**0,999**

The correlation coefficients R^2 (Table 2) indicate that the adsorption of uranium by the two materials studied follows pseudo-second-order kinetics, with values of $R^2 > 0,999$. According to Ho and McKay [52], this adsorption corresponds to chemisorption, involving the formation of valence bonds between the functional groups present on the surface of the materials and the uranyl ions [53].

3.8. Desorption and regeneration

In order to evaluate the reversibility of uranium sorption and the regeneration capacity of adsorbents, with the aim of making the adsorption process more economical and efficient, desorption experiments were carried out using different concentrations of nitric acid (0,01 N; 0,1 N; 0,2 N and 0,5 N) as desorbing solution, at room temperature. The desorption phase for a given cycle was carried out under the optimal conditions determined during the adsorption step. The results are presented in Figure 10.

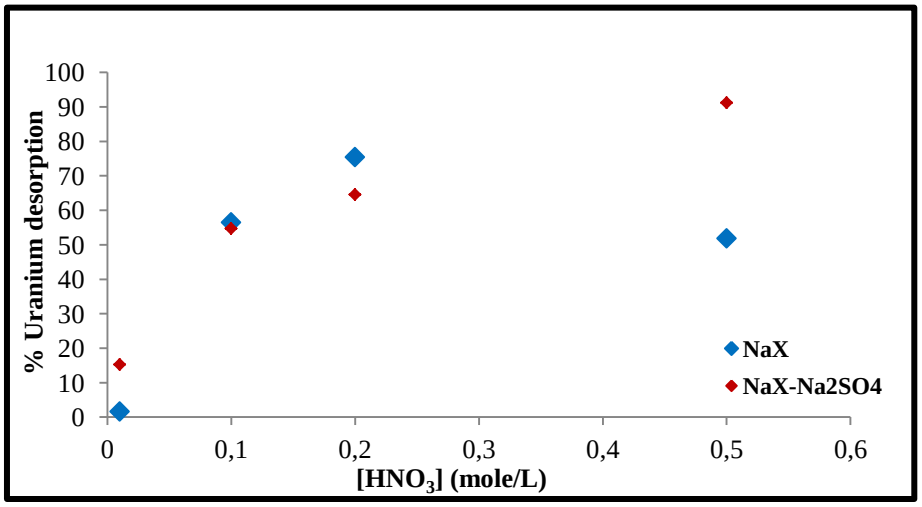

Fig 10. Effect of nitric acid concentration on the desorption efficiency of uranium on NaX and NaX-Na_2SO_4 zeolites.

The percentage of uranium desorption increases with increasing nitric acid concentration for both materials. The desorption percentages reach a maximum at respective HNO_3 concentrations of 0,2 N for NaX zeolite and 0,5 N for NaX-Na_2SO_4.

The desorption percentages for one treatment cycle are 75% for NaX and 91% for modified NaX. We can conclude that adsorption is a reversible process for both the processed and modified materials.

3.9. Application of the different materials developed in the treatment of a real effluent

The application of NaX and NaX-Na_2SO_4 materials in the recovery of uranium from uranium effluents from purification was carried out using the optimal adsorption conditions determined in this work on synthetic uranium solutions.

The adsorption efficiency of uranyl ions on NaX and NaX-Na_2SO_4 materials with a real solution titrating in 104,08 mgU/L is respectively of 29,29% and 64,11% for NaX and NaX-Na_2SO_4, these values are far compared to the adsorption efficiency of uranyl ions from a synthetic solution. This decrease in adsorption rate is probably due to the presence of other cations in the actual solution corresponding to the effect of competing ions such as iron (Fe^{2+}), magnesium (Mg^{2+}) and zinc (Zn^{2+}).

4. Conclusion

The main objective of this work is the preparation of porous adsorbents with a large specific surface area, high thermal stability, and capable of treating aqueous effluents contaminated by uranium.

The chemical modification of NaX zeolite by intra-synthesis, via the addition of sodium sulfate (Na_2SO_4), aimed to increase the density and reactivity of the active sites, thus improving both the selectivity and the adsorption capacity with respect to uranium.

NaX zeolite was successfully synthesized and then modified by incorporation of sodium sulfate (Na_2SO_4) hydrothermally to obtain a NaX–Na_2SO_4. X-ray diffraction (XRD) analysis confirmed that the crystallinity of the zeolite is preserved after modification. Infrared spectroscopy (FTIR) analysis confirmed the presence of the characteristic groups of the zeolite structure. BET analysis determined the specific surface area of the materials, revealing a slight decrease after modification, attributed to the incorporation of sodium sulfates into the porous structure. Thermogravimetric analysis (TGA) showed good thermal stability of both materials up to 800°C. The adsorption capacities were found to be in the order of 23 mgU/g for the NaX zeolite and 35 mgU/g for the NaX–Na_2SO_4.

The study of desorption with nitric acid (HNO_3) showed a recovery of uranyl ions of the order of 75% for the NaX material with a 0,2 N solution, and 91% for the NaX-Na_2SO_4 with 0,5 N HNO_3, after one treatment cycle.

The adsorption efficiency of uranyl ions from a real solution titrating 104,08 mg/L in uranium is approximately 29% for the NaX zeolite and 64% for the NaX-Na_2SO_4 . These results allow us to conclude that the NaX-Na_2SO_4 has a significantly higher adsorption capacity than the NaX parent zeolite.

Conflict of Interest

The authors declare that they have no conflict of interest.

References

1. International Atomic Energy Agency (IAEA). Operating experience with nuclear power stations in Member States. 2024 ed. Vienna (Austria): IAEA; 2024.
2. Khemaissia S, Abaidia R, Houhoune F, Bennemla M, Bayou N, Haddad D, Benturki A, Bendjeriou F, Zermane F. Synthesis and characterization of ZSM-12 zeolite for uranium (VI) adsorption: isotherm, kinetic, and thermodynamic investigations. *Comptes Rendus Chim*. 2025;28:79–93.
3. De Lurdes Dinis M, Fiúza A. Mitigation of uranium mining impacts: technologies groundwater remediation technologies. *Geosciences*. 2021;11:250.
4. Murukutti MK, Jena H. Synthesis of nano-crystalline zeolite-A and zeolite-X from Indian coal fly ash, its characterization and performance evaluation for the removal of Cs^{+} and Sr^{2+} from simulated nuclear waste. *J Hazard Mater*. 2022;423:127085.
5. Król M. Natural vs. synthetic zeolites. *Crystals*. 2020;10(7):1–8.
6. Baerlocher C, McCusker LB. Database of Zeolite Structures. International Zeolite Association; 2020.
7. Borel M. Synthèse de nano-cristaux de zéolithe Y stabilisé en absence d'agent organique structurant [thèse de doctorat]. Mulhouse (France): Université de Haute-Alsace; 2017.
8. Prates ARM. Hollow Beta zeolites: synthesis and impact of the hollow morphology on diffusion and catalysis [thèse de doctorat]. Lyon (France): Université de Lyon; 2019.
9. Maesen TLM, Marcus B. Introduction to zeolite science and practice. In: *Studies in Surface Science and Catalysis*. Amsterdam: Elsevier; 2001. Vol. 137, p.1078.
10. Lim WR, Yoshida K, Lee CH, Seo B. Radionuclide-specific ion exchange on zeolite frameworks: a conceptual proposal. *Sustain Mater Technol*. 2025;44:e01397.
11. Jiménez-Reyes M, Almazan-Sanchez PT, Solache-Ríos M. Radioactive waste treatments by using zeolites: a short review. *J Environ Radioact*. 2021;233:106610.
12. Ezzeddine Z, Batonneau-Gener I, Pouilloux Y, Hamad H, Saad Z. Synthetic NaX zeolite as a very efficient heavy metals sorbent in batch and dynamic conditions. *Colloids Interfaces*. 2018;2:22.
13. Gackowski M, Datka J. Acid properties of hierarchical zeolites. *Molecules*. 2020;25:1044.
14. Mohsin MZ, Huang J, Hussain MH, Zaman WQ, Liu Z, Rehman S, Zhuang Y, Guo M, Mohsin A. Revolutionizing bioremediation: advances in zeolite-based nanocomposites. *Coord Chem Rev*. 2023;491:215253.
15. Hasan MK, Ahsan S, Islam M, Beg MRA. Cation exchange and adsorptive properties of synthetic zeolites for heavy metal removal: mechanisms and mechanistic insights. *J Environ Chem Eng*. 2021;9(6):106307.
16. Tchemmou S, Gherbi A. Development of hierarchically porous zeolites: adsorbents for aqueous solution depollution [Master's thesis]. Tizi Ouzou (Algeria): Mouloud Mammeri University; 2018.
17. Laurent S, Bertrand G, Lapisardi G, Dulot H, De Grandi V, Minoux D, Dath JP. Catalyst usable in hydroconversion comprising at least one zeolite and group VIII and VIB metals, and preparation of the catalyst. *International Patent* WO 2013093229 A1. 2013.
18. Jia X, Khan W, Wu Z, Choi J, Yip ACK. Modern synthesis strategies for hierarchical zeolites: bottom-up versus top-down strategies. *Adv Powder Technol*. 2019;30(3):467–484.
19. Romero MD, Ovejero G, Rodriguez A, Gomez JM. Enhancement of the basic properties in FAU zeolites by impregnation with cesium hydroxide. *Microporous Mesoporous Mater*. 2005;81(1–3):313–320.
20. Abbas TK, Ibrahim ZH, Mustafa K, Al-Juboori RA, Nafae TM, Al-Mashhadani AH, Fal M, Alotaibi AM, Alsalhy QF. A modified zeolite (Na_2SO_4@zeolite NaA) as a novel adsorbent for radium-226,228 from acidic radioactive wastewater: synthesis, characterization and testing. *J Environ Chem Eng*. 2024;12(2):112197.
21. Snell FD. Photometric & fluorometric methods of analysis. New York: John Wiley & Sons; 1978.
22. Fritz J, John-Richard M. Colorimetric uranium determination with arsenazo. *Anal Chim Acta*. 1959;20:164–171.
23. Savvin SB. Analytical applications of arsenazo III. Part II: determination of thorium, uranium, protactinium, neptunium, hafnium and scandium. *Talanta*. 1964;11:1–6.
24. Treacy MMJ, Higgins JB. Collection of simulated XRD powder patterns for zeolites. Amsterdam: Elsevier; 2007.
25. Frost RL, Kloprogge JT. Fourier transform infrared (FTIR) study of the thermal dehydration of natural stilbite. *Spectrochim Acta A Mol Biomol Spectrosc.* 2002;58(13):2829–2836.
26. Wang S, Wu H. Environmental applications of zeolites. *Chemosphere*. 2009;74:150–160.
27. Liu J, Chen L, Cui H, Zhang J, Zhang L, Su CY. Applications of metal-organic frameworks in heterogeneous supramolecular catalysis. *Chem Soc Rev*. 2014;43(16):6011–6061.

28. Guo X, Song S, Zhu J. Removal of uranium (VI) from aqueous solution by sorption on zeolite. *J Radioanal Nucl Chem*. 2006;270:523–528.
29. Feng X, Zhu Y, Zhu J. Removal of uranium (VI) from aqueous solutions by natural zeolite. *J Environ Radioact*. 2007;97:85–92.
30. Shetty S, Nadagouda MN. Selective removal of uranium (VI) from aqueous solution using modified zeolites. *Sep Sci Technol*. 2020;55(7):1231–1242.
31. Abbas TK, Ibrahim ZH, Mustafa K. Synthesis and characterization of zeolite for removal of radionuclides from radioactive wastewater. *J Radioanal Nucl Chem*. 2020;325:593–603.
32. Han X, Chen L, Zhang J, Wang Y. Adsorption of uranium (VI) on modified zeolite: kinetics and thermodynamics. *J Environ Chem Eng*. 2020;8:103759.
33. Liu Y, Wang Y, Li J, Zhang X. Removal of uranium (VI) from aqueous solution using a novel zeolite-based adsorbent. *J Hazard Mater*. 2020;385:121600.
34. Wang S, Li Y, Liu Y. Adsorption of uranium (VI) from aqueous solution by modified zeolite: experimental and modeling study. *Chem Eng J*. 2017;327:455–464.
35. Zhang X, Guo J. Effect of pH on uranium (VI) adsorption onto natural zeolite. *J Environ Radioact*. 2010;101:861–865.
36. Liu J, Li Z, Wang Z. Adsorption behavior of uranium (VI) onto natural zeolite: kinetics and thermodynamics. *J Radioanal Nucl Chem*. 2015;305:295–302.
37. Saha B, Chowdhury S. Adsorption of uranium (VI) from aqueous solution by natural zeolite: effect of pH, temperature and ionic strength. *J Environ Radioact*. 2013;117:32–39.
38. Chen X, Wang X, Liu L. Synthesis and characterization of modified zeolite for uranium (VI) adsorption. *J Hazard Mater*. 2014;271:86–93.
39. Müller K, Brendler V, Foerstendorf H. Aqueous uranium (VI) hydrolysis species characterized by attenuated total reflection Fourier-transform infrared spectroscopy. *Inorg Chem*. 2008;47(21):10127–10134.
40. Zhu Y, Feng X, Zhu J. Adsorption of uranium (VI) from aqueous solution by natural zeolite: effect of temperature and ionic strength. *J Environ Radioact*. 2008;99:1145–1151.
41. Abbas TK, Ibrahim ZH, Mustafa K. Removal of uranium (VI) from radioactive wastewater using modified zeolite adsorbent. J *Radioanal Nucl Chem*. 2020;324:89–98.
42. Zhou L, Hu J. Adsorption of uranium (VI) onto natural zeolite: kinetic and thermodynamic studies. *J Environ Radioact*. 2012;103:12–18.
43. Kumar P, Singh V. Removal of uranium (VI) from aqueous solution by modified zeolite. *J Environ Chem Eng*. 2019;7:103270.
44. Zhang L, Wang Y. Effect of temperature on uranium (VI) adsorption onto zeolite. *J Radioanal Nucl Chem*. 2017;313:141–148.
45. Li J, Chen S, Wu Y. Adsorption of uranium (VI) from aqueous solution using natural zeolite: isotherm and kinetic studies. *J Environ Radioact*. 2011;102:1132–1137.
46. Abd El-Lateef HM. Adsorption of uranium (VI) from aqueous solution by zeolite synthesized from Egyptian kaolin. *J Radioanal Nucl Chem*. 2017;312:1207–1215.
47. Freundlich H. Over the adsorption in solution. *Z Phys Chem*. 1906;57:384–470.
48. Dubinin MM, Radushkevich LV. Equation of the characteristic curve of activated charcoal. *Chem Zent*. 1947;1:875–890.
49. Barkat M, Nibou D, Amokrane S, Chegrouche S, Mellah A. Uranium (VI) adsorption on synthesized 4A and P1 zeolites: equilibrium, kinetic, and thermodynamic studies. *C R Chim*. 2015;18:119–130.
50. Younes AA, Salem AR, El-Maghrabi HH, Rabie K, El-shereafy E. Magnetically modified hydroxyapatite nanoparticles for the removal of uranium (VI): preparation, characterization and adsorption optimization. *J Hazard Mater*. 2019;378:120703.
51. Fasfous I, Dawoud JN. Uranium (VI) sorption by multiwalled carbon nanotubes from aqueous solution. *Appl Surf Sci*. 2012;259:433–440.
52. Ho YS. Citation review of Lagergren kinetic rate equation on adsorption reactions. *Scientometrics*. 2004;59(1):171–177.
53. Bi C, Nian J, Zhang C, Liu L, Zhu L, Zhu R, Qi Q, Ma F, Dong H, Wang C. Efficient uranium adsorbent prepared by grafting amidoxime groups on dopamine modified graphene oxide. *Prog Nucl Energy*. 2023;155:104510.